

This is a repository copy of *The quest for the optimum angular-tilt of terrestrial solar panels or their angle-resolved annual insolation*.

White Rose Research Online URL for this paper:

<https://eprints.whiterose.ac.uk/157810/>

Version: Accepted Version

---

**Article:**

Schuster, Christian Stefano (2020) The quest for the optimum angular-tilt of terrestrial solar panels or their angle-resolved annual insolation. *Renewable Energy*. pp. 1186-1191. ISSN 0960-1481

<https://doi.org/10.1016/j.renene.2020.01.076>

---

**Reuse**

This article is distributed under the terms of the Creative Commons Attribution-NonCommercial-NoDerivs (CC BY-NC-ND) licence. This licence only allows you to download this work and share it with others as long as you credit the authors, but you can't change the article in any way or use it commercially. More information and the full terms of the licence here: <https://creativecommons.org/licenses/>

**Takedown**

If you consider content in White Rose Research Online to be in breach of UK law, please notify us by emailing [eprints@whiterose.ac.uk](mailto:eprints@whiterose.ac.uk) including the URL of the record and the reason for the withdrawal request.

---

1                                   The quest for the optimum angular-tilt  
2                                   of terrestrial solar panels  
3                                   or their angle-resolved annual insolation

---

4                                   Christian Stefano Schuster<sup>a</sup>

5                                   a - Department of Physics, University of York, Heslington, York, YO10 5DD, UK

6                                   Correspondence and requests for materials should be addressed to  
7                                   CSS (e-mail: chriss@physics.org)

8    ABSTRACT

9    Although solar energy is the fastest growing power technology, terrestrial solar panels  
10   typically fall behind their performance ratings established under standardised test-conditions.  
11   In particular, the angular-tilt of a panel can greatly affect its overall performance. Many studies  
12   thus aim to find the optimum tilt that maximises the annual insolation level. However, no  
13   widespread consensus has so far been found, partly because of different model assumptions  
14   applied. Here, a technique is proposed to use actual, historical solar spectra for the rigorous  
15   assessment of a panel's tilt at a specific site. By combining multiple, free-accessible satellite-  
16   retrieved data products, the total all-sky insolation levels are tracked with a minutely changing  
17   global (hemispherical) solar spectrum over many years. While time-resolved annual insolation  
18   profiles can considerably vary among each other, the solar angle-resolved profile turns out to  
19   be robust to climatic conditions and is even site-independent for latitude-tilted panels. These  
20   findings can potentially unlock innovative yield optimisation methods.

21   **Keywords:** Photovoltaics; Solar spectrum; Insolation; Clouds; Solar panel; Panel orientation

## 22 1. INTRODUCTION

23 While many plants naturally follow the motion of the Sun to maximise photosynthesis  
24 (heliotropism), most terrestrial solar energy systems do not. Hoyt Hottel already noticed in  
25 1941 that “artificial flat-plate converters of solar energy are too cheap to warrant being  
26 mounted to follow the sun but may profitably be tilted permanently towards the Equator” [1].  
27 Today, tracking systems are still seen as expensive and in need of maintenance, but they also  
28 require energy for their operation, are prone to heavy snow layers or storm damage and often  
29 not applicable for small scale systems – as they can be too heavy for rooftop applications, for  
30 example.

31 The question then arises for which angular-tilt the annual **incoming solar radiation** (insolation)  
32 is maximised for a planar surface. Though a simple sounding problem, it is a complicated  
33 exercise [2], because one needs to consider Earth’s rotation, obliquity, orbital eccentricity and  
34 revolution around the Sun in addition to the site’s geographical altitude, latitude and  
35 longitude.

36 As the optimum angular-tilt has been widely studied in the literature, Yadav and Chandel  
37 recently reviewed various calculation methods, algorithms and optimisation techniques [3].  
38 The authors compare the results of analytical, numerical and experimental methods in order  
39 to assess the suitability of a technique for a particular location. They conclude that the  
40 optimum tilt is very site-specific due to environmental factors and must be accurately  
41 determined by considering long-term observational datasets. In fact, Jacobson and Jadav  
42 estimated two very different optimum tilts for almost the same geographical latitude: 34° for  
43 London in the UK and 45° for Calgary in Canada [4]. Today, a data-driven approach is thus  
44 emerging as a standard practice. For example, Siraki and Pillay [5] considered monthly average  
45 daily insolation levels for five different latitudes (spaced 10° apart); Darhmaoui and Lahjouji

46 [6] averaged the daily global solar radiation over 4-years of datasets for 35 sites in the  
47 Mediterranean region; Rakovec et al. [7] interpolated the hourly measurements of 10-year  
48 long data sets for four distinct locations in Slovenia; Li and Lam [8] used the 10-minute  
49 averages of *half-secondly* irradiance measurements over the entire year 2004 for the City  
50 University of Hong Kong.

51 Some authors also have started to use the “typical meteorological year” (TMY) as a type of  
52 hourly solar resource data, in which the entirety of original multi-year solar radiation and  
53 meteorological data sets is condensed into one year's worth of the most usual conditions.  
54 However, albeit TMY data collections may enable to estimate the optimum angular-tilt for all  
55 major cities worldwide [4] and facilitate (online) PV performance estimations [9], they  
56 ultimately are auxiliary datasets and cannot reflect the nonlinear dynamics of a globally  
57 changing climate [10, 11, 12]. For example, the combination of recurring temperature  
58 extremes, higher atmospheric pollution levels, intensified water crisis and disastrous river  
59 dynamics [13] could affect solar power systems directly or indirectly by variations in the solar  
60 spectrum and zonal albedo.

61 In the end, the actual solar spectrum remains the key parameter to know, because all other  
62 parameters are directly or indirectly depending on it. While the sunshine received by a  
63 terrestrial solar panel is continuously changing due to Earth's rotation and revolution, it does  
64 also depend on the chemical composition and meteorological condition of the atmosphere –  
65 both being subject to fluctuations on a minutely time scale.

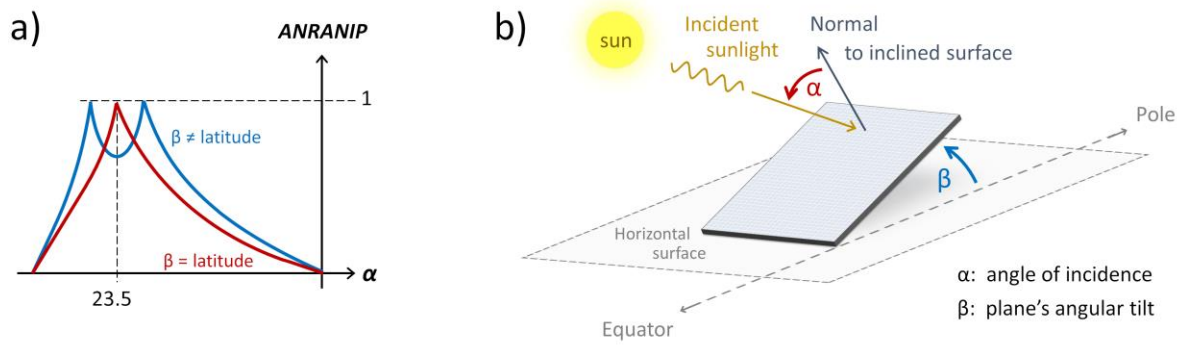
66 As datasets for the global solar spectrum are hardly available at this resolution, Bright et al.  
67 proposed to generate a synthetic time series stochastically from mean hourly weather  
68 observation data [14]. Although the model produces realistic irradiance profiles, it is of a non-

69 spatial nature and not intended to match real-world observational data. For example, the  
70 individual simulations at nearby locations would not correlate.

71 On the other hand, now more than 700 satellites are recording data for Earth observation  
72 purposes [15]. The National Aeronautics and Space Administration (NASA), as well as the  
73 European Space Agency (ESA), offer wide ranging resources down to 1 min time stamps. Why  
74 not combine such valuable information to model the global solar spectrum at a specific  
75 location?

76 Peters et al. recently initiated a few studies based on this approach [16, 17], but neglected  
77 most of the dynamic processes by considering only daily average values of a single-year and  
78 used scale-to-match procedures, indirectly derived parameters as well as the standardised  
79 extra-terrestrial spectrum (ASTM E490). The authors worked with the **Simple Model** of the  
80 **Atmospheric Radiative Transfer of Sunshine (SMARTS)** by C. Gueymard [18, 19], as the open-  
81 source program conveniently allows to include satellite retrieved data sets. However, if the  
82 time resolution of the modelled spectra is only dictated by the embedded data series,  
83 minutely changing atmospheric and meteorological conditions can always be included.

84 Here, by combining datasets from multiple, free-accessible satellite-product services, section  
85 2 shows how the incident solar spectrum can be tracked on a tilted plane for every minute  
86 over many years. This allows to accurately analyse in section 3 not only the insolation level as  
87 a function of the angular-tilt, but also its solar angle dependency. While time-resolved annual  
88 insolation profiles can considerably vary among each other, the **angle-resolved annual**  
89 **insolation profile (ANRANIP)**, as defined in Fig. 1, turns out to be robust to climatic changes  
90 and becomes even site-independent for latitude-tilted panels. These findings could potentially  
91 unlock innovative yield optimisation methods, as explained in section 4.



92

93 **Fig. 1.** The **angle resolved annual insolation profile (ANRANIP)**.

94 The *ANRANIP* shows **(a)** how the incident solar energy is dispersed over the angles of incidence  $\alpha$  for  
 95 an inclined surface;  $\alpha$  is defined as positive if measured from the surface normal to Sun's position **(b)**.

96 The *ANRANIP* depends on the plane's angular tilt  $\beta$ , measured from Earth's ground, and is normalised  
 97 to its global peak value.

## 98 2. METHODS

99 The spectra are calibrated to the actual measured extra-terrestrial irradiance *TOA* at the top  
 100 of Earth's atmosphere. Since the so calculated clear-sky global spectrum *CSGTI* on a tilted  
 101 plane differs from the total all-sky irradiance *GTI*, e.g. due to clouds, it must be multiplied  
 102 with the clear-sky index  $\sigma$ ,

$$103 \quad GTI = \sigma \cdot CSGTI \quad \text{with } \sigma = \frac{GHI}{CSGHI}. \quad (1)$$

104 The clear-sky index  $\sigma$  is defined as the ratio of the measured global horizontal irradiance *GHI*  
 105 and the computed clear-sky global irradiance *CSGHI* on a horizontal plane. Since  $\sigma$  is  
 106 independent of tilt and orientation, i.e. independent on solar geometry [20], the transposition  
 107 from a horizontal ( $\beta = 0^\circ$ ) to tilted surface ( $\beta > 0^\circ$ ) can be performed by setting  $\frac{GTI}{CSGTI} = \frac{GHI}{CSGHI}$ ,

108 which yields Eq. 1. Finally, records for *TOA*, *GHI* and *CSGHI* are freely available from the

109 **Copernicus Atmosphere Monitoring Service (CAMS)** [21], thus  $\sigma$  and hence *GTI* are readily

110 calculated from SMARTS output data, see Tab. 1. CAMS is the European Union’s contribution  
 111 to the **Global Earth Observation System of Systems (GEOSS)**; it is delivering geospatial  
 112 information from  $-66^\circ$  to  $66^\circ$  in both latitudes and longitudes since February 2004 – with a  
 113  $0.5^\circ$  spatial and up to one-minute temporal resolution.

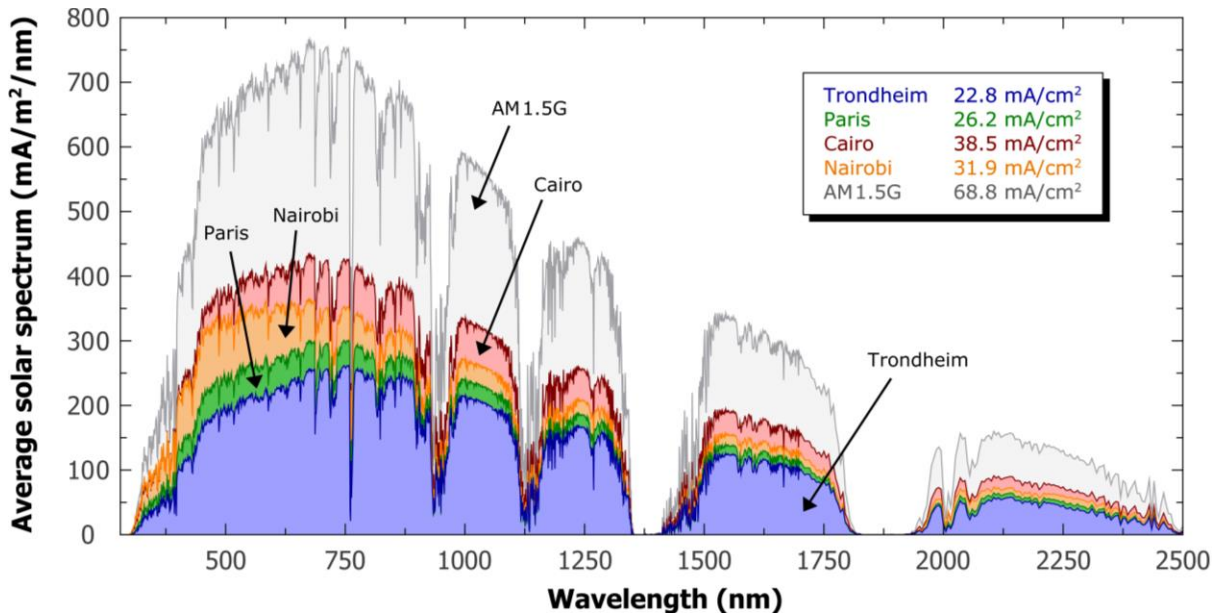
input to SMARTS	output from SMARTS
location (latitude, longitude, altitude), date and time (UTC)	angle of incidence $\alpha$
angular-tilt $\beta$ of solar panel (facing toward Equator)	clear-sky global irradiance for a tilted plane ( <i>CSGTI</i> )
temperature, relative humidity, surface pressure [22]	clear-sky global solar spectrum for a tilted plane
total precipitable water column [23]	
CO <sub>2</sub> concentration [24, 25], total-column abundance of ozone [26]	
ground albedo of a light soil (non-Lambertian reflectance)	
aerosol type and tropospheric pollution level [27]	
extra-terrestrial irradiance on top of Earth’s atmosphere [21]	

114 **Tab. 1.** A list of the required data (left) for the relevant output parameters from SMARTS (right).  
 115 For a tilted plane, the all-sky solar spectrum *G<sub>T</sub>* is derived with a 1 nm spectral and 1 min temporal  
 116 resolution from the modelled clear-sky spectrum *CSGTI* via the clear-sky index  $\sigma$  [21]. All referenced  
 117 quantities are based on freely accessible data sets gathered from satellites. As the time step is 24h for  
 118 [23, 26], 12h for [24, 25] and 3h for [27], the data were first interpolated to the one-minute resolution  
 119 of the series [21, 22]. Measurements of the total optical depth and partial optical depths of the major  
 120 atmospheric species – dust, sea salt, black carbon and organic matter – were used to select the correct  
 121 aerosol type and its tropospheric pollution level via the established McClear model from Lefèvre et al.  
 122 [28].

### 123 3. RESULTS

124 In this paper, the cities Trondheim (Norway), Paris (France), Cairo (Egypt) and Nairobi (Kenya)  
 125 are chosen as a representative set for the distinctive climatic characteristics on Earth. Yet,  
 126 before analysing their insolation levels, it is instructive to compare their modelled spectra with  
 127 the AM 1.5G standard solar spectrum from NREL [29], since it is widely used in the literature

128 and for the benchmarking of solar cells. For this comparison, the average of all non-zero  
 129 spectra of a 14-year long time series was taken to highlight the overall effects and the  
 130 differences to the spectral standard, see Fig. 2.



131

132 **Fig. 2.** A comparison of long-time averaged solar spectra at distinct climatic locations.

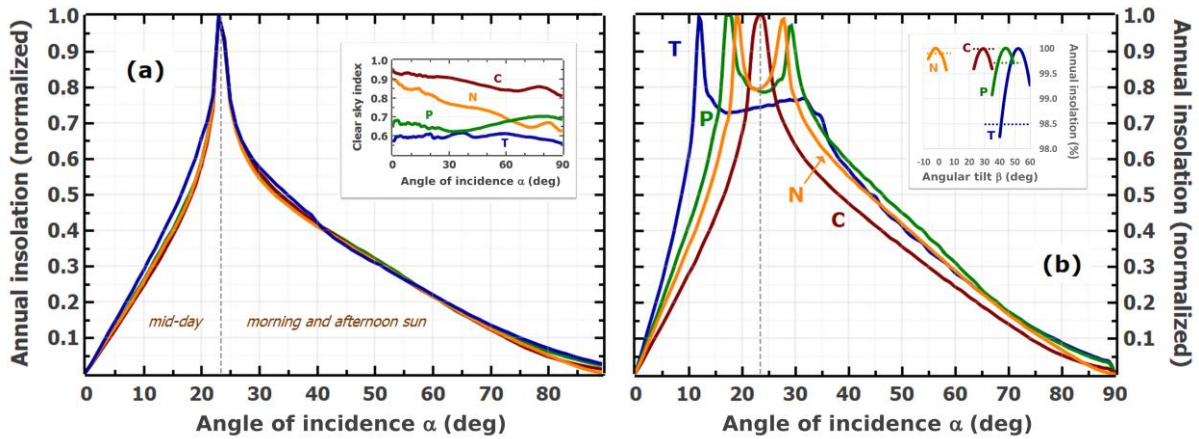
133 For each city, the 14-year time series of non-zero historical solar spectra at one-minute intervals was  
 134 averaged and expressed as electrical current density. The global standard AM 1.5G spectrum from  
 135 NREL [29] is shown for comparison, highlighting the differences to a typical solar spectrum received by  
 136 a latitude-tilted surface in the outdoors. The inset quotes the total currents after integrating from 280  
 137 to 4000 nm wavelength. Since a time-series of solar spectra cannot be adequately represented in a  
 138 single graph, the average spectrum was chosen as the most appropriate quantity of comparison.

139

140 Whereas the spectrum of Nairobi qualitatively experiences the greatest energy loss in the near  
 141 infra-red, the spectra of Trondheim and Paris suffer the most in the visible range; the spectrum  
 142 of Cairo instead resembles most the AM 1.5G standard, because it apparently differs from it  
 143 just by a scaling factor of 0.6.



144 While the direct comparison to the average spectra might first not seem fair, it does highlight  
 145 the great degree of idealisations set out for the AM 1.5G standard. For example, it was defined  
 146 for normal incident sunlight (of a clear sky), but which is the least likely condition for a fix-  
 147 tilted panel, according to Fig. 3.



148  
 149 **Fig. 3.** A comparison of the normalised angle-resolved annual insolation levels for the investigated  
 150 cities Trondheim (T), Paris (P), Cairo (C) and Nairobi (N).

151 All latitude-tilted panels (a) exhibit the same angle-resolved annual insolation profile (*ANRANIP*) from  
 152 year-to-year, despite being subject to different environments (see inset). In contrast, if panels are tilted  
 153 to maximise annual yield (b), the *ANRANIP* becomes site-dependent and exhibits two maxima. The  
 154 inset shows that major differences to the optimum case appear at high-latitude locations (up to 1.5%  
 155 in absolute), with the dotted lines corresponding to the insolation levels of latitude-tilted planes. Here,  
 156 the all-sky *G<sub>Tl</sub>* as a function of  $\alpha$  is found via SMARTS from a minutely time series of reconstructed,  
 157 historical global solar spectra from 2004 to 2018, see Eq. 1 and Tab. 1. All *G<sub>Tl</sub>* values with the same  
 158 angle of incidence  $\alpha$  (rounded to the nearest integer) are added together irrespective of their  
 159 timestamps, before the resulting graph is normalised to its peak value.

160 Please note, Fig. 3 does *not* suggest that a panel's optimum angular tilt is  $\beta = 23.45^\circ$ . Instead,  
 161 it points out that the area of a panel receives most energy from Sun at an angle-of-incidence

162  $\alpha = 23.45^\circ$ , if and only if it is mounted at latitude-tilt, regardless of atmospheric changes, the  
163 climatic conditions or its geographical location. In fact, since latitude-tilted surfaces are  
164 parallel to a horizontal plane at the Equator, they experience the same apparent motion of  
165 the Sun: sunlight is received under an angle of  $\alpha = 23.45^\circ$  twice a day and once at solstice,  
166 whereas the normal incidence ( $\alpha = 0^\circ$ ) only occurs at the equinoxes (at solar noon). By  
167 analysing the most frequent condition of photovoltaic module technologies, Bora et al. [30]  
168 indicate that the *ANRANIP* of a latitude-tilted surface indeed peaks at  $\alpha = 23.45^\circ$ , i.e. at Earth's  
169 obliquity.

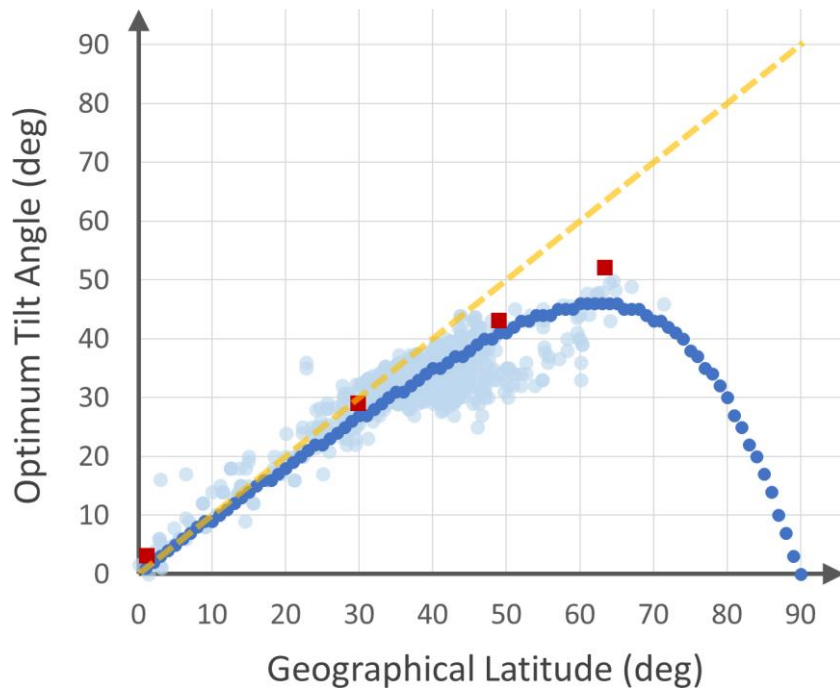
170 For angular-tilts  $\beta$  smaller than the latitude angle, the insolation is received at lower (higher)  
171 angles of incidence in the summer (winter) periods. In effect, the two days with the minimum  
172 angle of incidence move from the equinoxes toward the summer solstice. If they merge, the  
173 smallest angle of incidence would only occur once a year. In addition, as the incident angles  
174 on the solstices differ from  $23.45^\circ$  and from each other (at solar noon), the *ANRANIP* of a non-  
175 latitude-tilted surface has two maxima, evenly spread around  $23.45^\circ$ . The spread is given by  
176 the difference between the latitude and selected tilt. Finally, for tilts even smaller than the  
177 difference between the latitude and polar circle ( $66.55^\circ$ ), no insolation will be received at all  
178 on certain winter days.

#### 179 4. DISCUSSION

180 The quest for the optimum angular-tilt of a terrestrial solar panel might not solely be resolved  
181 by maximising its annual insolation level, because it may not necessarily lead to the maximum  
182 output of a solar energy system [31] – regardless of the solar resource data used.

183 Firstly, the (local) foreground albedo seen by a tilted surface changes over time [32], which is  
184 a key factor in ice- and snowscapes, yet many authors still assume a *constant* foreground

185 albedo of 0.20 (typical grassland), often equal to the zonal albedo used for the backscattering  
186 calculations. The so derived optimised tilts will likely be incorrect [7, 32], because the local  
187 and zonal albedo have a spectral and unequal dependency as the ground surface is rarely  
188 uniform over large areas. Secondly, modules can get immersed in fog (smog) or partly covered  
189 by ice, snow, hardened dust, sand, dirt, pollen, leaves or bird droppings; they can become  
190 prone to fungi and mildew [33] and be permanently damaged by hail [34], frost [35] or even  
191 a shadow if monolithically integrated [36, 37, 38, 39]. Solar panels also undergo daily heat and  
192 cold cycles, as they inevitably age. Consequently, many environmental factors have a major  
193 impact on the useful energy output of a solar energy system over its operational lifetime.  
194 Their effects tend to lessen with higher angular-tilts, as the greater the tilt, the more debris  
195 can drop down or be washed away by rain, but also the cooler the panel's temperature [40],  
196 which leads to increases in the energy yield. From this perspective, the latitude-tilt would be  
197 a better choice, because it is often found to be greater than the optimum tilt according to Fig.  
198 4, with a reduction in annual insolation of ca. 1.5% at most according to Tab. 2. However, the  
199 land costs, any space and mounting constraints or compliances with building regulations  
200 might also influence a panel's tilt.



201

202 **Fig. 4.** The optimum angular-tilt that maximises the annual insolation on a flat plane.

203 It is a function of the geographical latitude among other factors, implied by the large spread of  
 204 literature data (light coloured symbols) [31, 8, 7, 5, 6, 41, 42, 43, 4]. The dark coloured (round) symbols  
 205 refer to the optimum-tilted plane if environmental factors were negligible. The square dots stand for  
 206 the here investigated cities Trondheim (63.4°), Paris (49.0°), Cairo (29.9°) and Nairobi (-1.2°), whose  
 207 optimum angular-tilts are based on a minutely time series of reconstructed, historical global solar  
 208 spectra between February 2004 and February 2018.

City	Country	Latitude	Longitude	Altitude	ASPD	Annual Insolation Level	
						@Latitude	@Optimum
Trondheim	Norway	63°26′	10°28′	263 m	9:40 h	1143	1161 (52°)
Paris	France	48°58′	2°38′	92 m	10:44 h	1485	1490 (43°)
Cairo	Egypt	29°56′	31°40′	284 m	11:20 h	2342	2342 (29°)
Nairobi	Kenya	-1°11′	36°55′	1796 m	11:39 h	2043	2045 (3°)

209 **Tab. 2.** A comparison of sunshine duration and insolation levels for four distinct climatic locations.  
210 The annual insolation level is given in kWh/m<sup>2</sup> for a surface at latitude tilt (left column) and at optimum  
211 angular-tilt (right column). The optimum tilt (quoted in brackets) is derived from non-zero historical,  
212 global (hemispherical) solar spectra at 1 min intervals between 2004 and 2018. *ASPD* refers to the  
213 **Average Sunshine Per Day** with the average taken over the same period (2004-2018). For Nairobi, the  
214 optimum tilt is found slightly higher than the latitude angle and with the panel facing away from the  
215 Equator – in agreement with Jacobson and Jadhav [4]. The annual insolation, as a time and spectrally  
216 integrated quantity, is not significantly affected by seasonal weather fluctuations (see Supplementary  
217 Fig. S1).

218 If environmental factors and installation restraints prevent a clear definition or application of  
219 the optimum angular-tilt, the annual insolation level might instead be best exploited by the  
220 inverse approach: for a given angular-tilt, the panel's reflection properties are optimised to its  
221 *ANRANIP*, as it mostly depends on astronomical factors.

222 Weather effects can be seen as a source of superimposed noise, which is effectively averaged  
223 out. Accordingly, the insolation received at a certain angle of incidence is more robust to  
224 climatic influences, whereas a time-resolved insolation profile can considerably vary from year  
225 to year. For example, while a latitude-tilted panel at Nairobi received almost 40% less  
226 insolation in June 2008 with reference to its monthly average (see Supplementary Fig. S2), the  
227 angle-resolved insolation only exhibits a 6% deviation at most (see Supplementary Fig. S3 and  
228 S4). The perspective of how yield can be maximised thus may change, when the panel's

229 *ANRANIP* is considered in the analysis. In fact, independent of the geographical location, all  
230 latitude-tilted panels have the same *ANRANIP* with the greatest deviations only occurring near  
231 the peak position, i.e. at an angle of incidence of 23.45°.

232 In summary, variations in the solar spectrum may play a crucial role in the future asset of solar  
233 energy technologies, such as the emerging perovskite-on-silicon tandem cell or other novel  
234 multi-junction approaches. For this purpose, a rigorous modelling technique is proposed for  
235 retrieving actual solar spectra at one-minute intervals, using free-accessibly satellite product  
236 services, such as the SoDa-pro platform. Here, the four cities Trondheim (Norway), Paris  
237 (France), Cairo (Egypt) and Nairobi (Kenya) were chosen as a representative set for four  
238 different climatic zones on Earth. By tracking the incident global solar spectra from 2004 to  
239 2018, their spectral, temporal and solar-angle resolved insolation profiles are accurately  
240 analysed as a function of the panel's angular-tilt. Only small differences in the total insolation  
241 levels could thereby be found between optimum and latitude tilted panels (with ca. 1.5% at  
242 most). However, since the angle-resolved annual insolation is far less sensitive to weather  
243 dynamics than a time-resolved profile, a panel's energy yield can always be increased for any  
244 given angular-tilt by adapting its anti-reflection properties to its *ANRANIP*. This practice  
245 reduces not only unnecessary reflection losses but also the risk of visual distress to pilots (e.g.  
246 flash blindness or veiling) near airports or high rises. In addition, the panel's yield optimisation  
247 would become decoupled from the considerations of mounting practicalities or building  
248 regulations. Since the *ANRANIP* allows to quantify how much solar energy falls from where  
249 onto a façade, wall or glass window over a calendar year, it could be applied as a simple but  
250 effective architectural design tool for passive solar buildings.

## 251 5. ACKNOWLEDGEMENTS

252 This research did not receive any specific grant from funding agencies in the public,  
253 commercial, or not-for-profit sectors. Thanks are given to Andrea Canino, Alberto Jimenez,  
254 Stefan Kremer, Kezheng Li, Manuel Mendes, Claudio Padilha, Dario Rapisarda, Mark Scullion  
255 and Brian Smith for their thorough and helpful critiques. The author wants to thank the  
256 Institute of Physics for the carer and beneficiary fund, but also to Sara Castillo Avila for her  
257 patience, encouragements and continuous support over the past two years, in particular.

## 258 6. ADDITIONAL INFORMATION

259 **Competing interests:** The author declares no competing financial and non-financial interests  
260 in relation to the work described.

## 261 7. REFERENCES

262

- [1] H. C. Hottel, "Artificial Converters of Solar Energy," *Sigma Xi Quarterly*, vol. 29, no. 1, pp. 49-60, 1941.
- [2] R. E. Gabler, J. F. Petersen, L. M. Trapasso and D. Sack, *Physical Geography*, Brooks/Cole, 2009.
- [3] A. K. Yadav and S. S. Chandel, "Tilt angle optimization to maximize incident solar radiation: A review," *Renewable and Sustainable Energy Reviews*, vol. 23, p. 503–513, 2013.
- [4] M. Z. Jacobson and V. Jadhav, "World estimates of PV optimal tilt angles and ratios of sunlight incident upon tilted and tracked PV panels relative to horizontal panels," *Solar Energy*, vol. 169, pp. 55-66, 2018.
- [5] A. G. Siraki and P. Pillay, "Study of optimum tilt angles for solar panels in different latitudes for urban applications," *Solar Energy*, vol. 86, p. 1920–1928, 2012.
- [6] H. Darhmaoui and D. Lahjouji, "Latitude Based Model for Tilt Angle Optimization for Solar Collectors in the Mediterranean Region," *Energy Procedia*, vol. 42, p. 426 – 435, 2013.
- [7] J. Rakovec, K. Zakšek, K. Brecl, D. Kastelec and M. Topič, "Orientation and Tilt Dependence of a Fixed PV Array Energy Yield Based on Measurements of Solar Energy and Ground Albedo – a Case Study of Slovenia," *InTech, Energy Management Systems*, 2011.

- [8] D. H. Li and T. N. T. Lam, "Determining the Optimum Tilt Angle and Orientation for Solar Energy Collection Based on Measured Solar Radiance Data," *International Journal of Photoenergy*, vol. 2007, no. 85402, 2007.
- [9] A. P. Dobos, "PVWatts Version 5 Manual," *Technical Report*, no. NREL/TP-6A20-6264, 2014.
- [10] V. Masson-Delmotte, P. Zhai, H. O. Pörtner, D. Roberts, J. Skea, P. R. Shukla, A. Pirani, W. Moufouma-Okia, C. Péan, R. Pidcock, S. Connors, J. B. R. Matthews, Y. Chen, X. Zhou, M. I. Gomis, E. Lonnoy, T. Maycock, M. Tignor and T. Waterfield, Eds. "IPCC Special Report on the impacts of global warming of 1.5°C," *World Meteorological Organization*, 2018.
- [11] J. C. Rocha, G. Peterson, Ö. Bodin and S. Levin, "Cascading regime shifts within and across scales," *Science*, vol. 362, no. 6421, p. 1379–1383, 2018.
- [12] P. B. Duffy, C. B. Field, N. S. Diffenbaugh, S. C. Doney, Z. Dutton, S. Goodman, L. Heinzerling, S. Hsiang, D. B. Lobell, L. J. Mickley, S. Myers, S. M. Natali, C. Parmesan, S. Tierney and A. P. Williams, "Strengthened scientific support for the Endangerment Finding for atmospheric greenhouse gases," *Science*, vol. 363, no. 6423, 2018.
- [13] P. Wester, A. Mishra, A. Mukherji and A. B. Shrestha, Eds., "The Hindu Kush Himalaya Assessment", Springer, Cham, 2019.
- [14] J. Bright, C. J. Smith, P. G. Taylor and R. Crook, "Stochastic generation of synthetic minutely irradiance time series derived from mean hourly weather observation data," *Solar Energy*, vol. 115, p. 229–242, 2015.
- [15] *Union of Concerned Scientists (UCS), the Satellite Database*, <https://www.ucsusa.org/nuclear-weapons/space-weapons/satellite-database>, UCS.
- [16] I. M. Peters and T. Buonassisi, "Energy Yield Limits for Single-Junction Solar Cells," *Joule*, vol. 2, pp. 1-11, 2018.
- [17] I. M. Peters, H. Liu, T. Reindl and T. Buonassisi, "Global Prediction of Photovoltaic Field Performance Differences Using Open-Source Satellite Data," *Joule*, vol. 2, p. 307–322, 2018.
- [18] C. Gueymard, "Parameterized Transmittance Model for Direct Beam and Circumsolar Spectral Irradiance," *Solar Energy*, vol. 71, no. 5, pp. 325-346, 2001.
- [19] C. Gueymard, "SMARTS, A Simple Model of the Atmospheric Radiative Transfer of Sunshine: Algorithms and Performance Assessment," *Professional Paper FSEC-PF-270-95. Florida Solar Energy Center, 1679 Clearlake Road, Cocoa, FL 32922*, 1995.
- [20] B. Elsinga, "Chasing the Clouds: Irradiance Variability and Forecasting for Photovoltaics," *PhD Dissertation, Utrecht University Repository*, 2017.
- [21] *CAMS Radiation Service, SoDa platform*, <http://www.soda-pro.com/web-services>.
- [22] *MERRA-2 RE-ANALYSIS, SoDa platform*, <http://www.soda-pro.com/web-services>, NASA.
- [23] *Vertical Integrated Water Vapour - Multimission*, © (2018) EUMETSAT, <https://navigator.eumetsat.int/product/EO:EUM:CM:MULT:HTW>.



- [24] AIRS Science Team/Joao Teixeira (2009), *AIRS/Aqua L3 Daily CO2 in the free troposphere (AIRS+AMSU) 2.5 degrees x 2 degrees V005, Greenbelt, MD, USA, Goddard Earth Sciences Data and Information Services Center (GES DISC), August 2018.*
- [25] AIRS Science Team/Joao Teixeira (2009), *AIRS/Aqua L3 Daily CO2 in the free troposphere (AIRS-only) 2.5 degrees x 2 degrees V005, Greenbelt, MD, USA, Goddard Earth Sciences Data and Information Services Center (GES DISC), August 2018.*
- [26] Pepijn Veefkind (2012), *OMI/Aura Ozone (O3) DOAS Total Column L3 1 day 0.25 degree x 0.25 degree V3, Greenbelt, MD, USA, Goddard Earth Sciences Data and Information Services Center (GES DISC), August 2018.*
- [27] CAMS-AOD, SoDa platform, <http://www.soda-pro.com/web-services>.
- [28] M. Lefèvre, A. Oumbe, P. Blanc, B. Espinar, B. Gschwind, Z. Qu, L. Wald, M. Schroedter-Homscheidt, C. Hoyer-Klick, A. Arola, A. Benedetti, J. W. Kaiser and J.-J. Morcrette, "McClear: a new model estimating downwelling solar radiation at ground level in clear-sky conditions," *Atmos. Meas. Tech.*, vol. 6, pp. 2403-2418, 2013.
- [29] NREL, *Reference Solar Spectral Irradiance: Air Mass 1.5 (2018)*, <https://rredc.nrel.gov/solar//spectra/am1.5/>.
- [30] B. Bora, O. S. Sastry and B. Prasad, "Seasonal analysis of most frequent condition and energy rating of PV module technologies," *Proceedings of the 32nd European Photovoltaic Solar Energy Conference and Exhibition*, no. 5BV.4.22, pp. 2237-2239, 2016.
- [31] C. B. Christensen and G. Barker, "Effects of Tilt and Azimuth on Annual Incident Solar Radiation for United States Locations," *Proceedings of Solar Forum 2001, Solar Energy: The Power to Choose*, 2001.
- [32] M. Gul, Y. Kotak, T. Muneer and S. Ivanova, "Enhancement of Albedo for Solar Energy Gain with Particular Emphasis on Overcast Skies," *Energies*, vol. 11, no. 2881, 2018.
- [33] A. Einhorn, L. Micheli, D. C. Miller, L. J. Simpson, H. R. Moutinho, B. To, C. L. Lanaghan, M. T. Muller, S. Toth, J. J. John, S. Warade, A. Kottantharayil and C. Engtrakul, "Evaluation of Soiling and Potential Mitigation Approaches on Photovoltaic Glass," *IEEE Journal of Photovoltaics*, 2018.
- [34] W. Muehleisen, G. C. Eder, Y. Voronko, M. Spielberger, H. Sonnleitner, K. Knoebl, R. Ebner, G. Ujvari and C. Hirschl, "Outdoor detection and visualization of hailstorm damages of photovoltaic plants," *Renewable Energy*, vol. 118, pp. 138-145, 2017.
- [35] R. Fillion, A.R.Riahi and A.Edrissy, "A review of icing prevention in photovoltaic devices by surface engineering," *Renewable and Sustainable Energy Reviews*, vol. 32, pp. 797-809, 2014.
- [36] T. J. Silverman, M. G. Deceglie, X. Sun, R. L. Garris, M. A. Alam, C. Deline and S. Kurtz, "Thermal and Electrical Effects of Partial Shade in Monolithic Thin-Film Photovoltaic Modules," *IEEE Journal of Photovoltaics*, vol. 5, no. 6, pp. 1742-1747, 2015.

- [37] T. J. Silverman, L. Mansfield, I. Repins and S. Kurtz, "Damage in monolithic thin-film photovoltaic modules due to partial shade," *IEEE Journal of Photovoltaics*, vol. 6, no. 5, pp. 1333-1338, 2016.
- [38] T. Silverman and I. Repins, "Shadows from People and Tools Can Cause Permanent Damage in Monolithic Thin-Film Photovoltaic Modules," *Proceedings of the 33rd European Photovoltaic Solar Energy Conference and Exhibition*, no. 5CO.6.6, 2017.
- [39] T. J. Silverman and I. Repins, "Partial Shade Endurance Testing for Monolithic Photovoltaic Modules," *7th World Conference on Photovoltaic Energy Conversion in Waikoloa Village, Hawaii*, 2018.
- [40] S. Khanna, K. Reddy and T. K. Mallick, "Performance analysis of tilted photovoltaic system integrated with phase change material under varying operating conditions," *Energy*, vol. 133, pp. 887-899, 2017.
- [41] J.-T. Brethouwer, W. v. Harten, S. Klootwijk and S. Visser, "Evaluation of radiation measurements for solar panel yield," *KNMI, Internal Report IR-2016-11*, 2016.
- [42] S. Y. Alsadi, Y. F. Nassar and K. A. Amer, "General Polynomial for Optimizing the Tilt Angle of Flat Solar Energy Harvesters Based on ASHRAE Clear Sky Model in Mid and High Latitudes," *Energy and Power*, vol. 6, no. 2, pp. 29-38, 2016.
- [43] S. Y. Alsadi and Y. F. Nassar, "A Numerical Simulation of a Stationary Solar Field Augmented by Plane Reflectors: Optimum Design Parameters," *Smart Grid and Renewable Energy*, vol. 8, pp. 221-239, 2017.

263

264